
Continual Learning in Open-vocabulary Classification with Complementary Memory Systems

Zhen Zhu*

Department of Computer Science
 University of Illinois at Urbana-Champaign
 zhenzhu4@illinois.edu

Weijie Lyu*

Department of Computer Science
 University of Illinois at Urbana-Champaign
 wlyu3@illinois.edu

Yao Xiao

Department of Computer Science
 University of Illinois at Urbana-Champaign
 yaox11@illinois.edu

Derek Hoiem

Department of Computer Science
 University of Illinois at Urbana-Champaign
 dhoiem@illinois.edu

Abstract

We introduce a method for flexible continual learning in open-vocabulary image classification, drawing inspiration from the complementary learning systems observed in human cognition. We propose a “tree probe” method, an adaption of lazy learning principles, which enables fast learning from new examples with competitive accuracy to batch-trained linear models. Further, we propose a method to combine predictions from a CLIP zero-shot model and the exemplar-based model, using the zero-shot estimated probability that a sample’s class is within any of the exemplar classes. We test in data incremental, class incremental, and task incremental settings, as well as ability to perform flexible inference on varying subsets of zero-shot and learned categories. Our proposed method achieves a good balance of learning speed, target task effectiveness, and zero-shot effectiveness. Code will be available [here](#).

1 Introduction

We would like image classification models that competently perform any arbitrary classification tasks and improve with each new example. By learning to match images to corresponding text, open-vocabulary image classifiers such as CLIP [1] can perform arbitrary “zero-shot” tasks, assigning each image to the category that best matches from among a set of options. Performance for a target task can be improved, for example, by training a linear classifier (or “linear probe”) with the model’s image features and new image/label pairs (“exemplars”). But it is not clear how to maintain the flexibility of the original model while learning from new examples.

We are inspired by the flexibility of human learning and inference. Humans consolidate vast experiences and observations but can also learn on the fly. For example, a child on a walk may initially identify a blue jay and robin and, after being shown a cardinal, identify one a few minutes later. Flexibility in human learning is enabled by complementary learning systems [2]: some slowly consolidate many experiences to enable fast inference without conscious effort, while others file individual observations and episodes for anytime retrieval and use. How can we make computer learning systems that likewise benefit from consolidated memory systems and exemplar-based memory to continually learn with zero-shot inference ability?

*These authors contributed equally to this work.

We investigate in the context of open-vocabulary image classification, using CLIP as the consolidated model. One challenge is to create exemplar-based memory systems that are performant in both accuracy and learning time (Sec. 3.3). A linear probe can achieve good accuracy, but learning from a new example requires $\mathcal{O}(n)$ time, where n represents the total number of exemplars. K-nearest neighbor can learn in $\mathcal{O}(1)$ time but tends to be less accurate than linear probe. Based on local linear models from the lazy learning literature [3], we propose a “tree probe” method that hierarchically clusters examples and trains linear models for each cluster. The time to learn from a new example is $\mathcal{O}(\log n)$, and the accuracy is close to linear probe.

A second challenge is to predict using both CLIP and exemplar-based models (Sec. 3.4). The exemplar-based model tends to perform well when an image’s label is “exemplar-covered”, i.e. the exemplar set contains at least one instance with the same label, while the consolidated model can potentially predict any label. At test time, we may not know whether the label of a given test image is exemplar-covered. Our idea is to use CLIP to estimate the probability that an image’s label is exemplar-covered and use that probability to weight the predictions of the two models.

Our experiments (Sec. 4) test flexible continual learning in the forms of data-incremental, class-incremental, and task-incremental learning, as well as flexible inference with categorization tasks that involve some, all, or none of the exemplar-covered labels. Our proposed methods to predict from exemplars and combine exemplar-based and consolidated models are surprisingly effective. In summary, the reader may benefit from the following **paper contributions**:

- Tree-probe exemplar model: Our locally linear models using a hierarchical clustering can be considered a member of the long-studied lazy learning approaches [3], but we are not aware of this specific method being proposed or used. Tree-probe has logarithmic-complexity training time in number of training samples and achieves better accuracy than nearest neighbor approaches. This can be attractive for interactive search, active learning, and other applications where annotated examples are received in a trickle and fast learning is required.
- Exemplar and consolidated model combination with embeddings: Our approach, to use the consolidated model to estimate applicability of the exemplar model and to combine model predictions in the label embedding space, enables effective continual open-vocabulary learning and performs significantly better than alternatives we tested.
- Flexible learning/inference experiments: Our experimental setup evaluates both the ability to continually learn from new samples and to flexibly apply those learnings to various category sets. This may provide a useful test framework for researchers seeking to further improve open-vocabulary continual learning.

2 Related works

2.1 Instance-based learning (IBL)

Instance-based learning (IBL) [4] is a family of learning algorithms that construct a decision boundary using a memory of training instances, allowing for efficient and flexible adaptation to new data points. This learning paradigm relies on the principle of local approximation, where predictions are made based on the stored instances that are most similar to the query. One of the most well-known IBL methods is the k -Nearest Neighbors (KNN) algorithm, which has been extensively studied for its simplicity and effectiveness in various domains, including classification and regression tasks [5–8].

Closely related to IBL is *lazy learning*, in which training data is organized for prediction at inference time instead of training time. This approach can be more practical than batch or “eager” learning in applications like online recommendation systems, when the training data is constantly evolving. Lazy learning approaches can include KNN or locally linear regression [9] or classification models [4], where models are trained based on neighbors to the query.

We investigate KNN, a form of locally linear classifiers, and globally linear classifiers, exploring their trade-offs for training and inference time and accuracy on a growing set of exemplars, as well as how to combine their predictions with a static image-language foundation model.

2.2 Open-vocabulary classification

Open-vocabulary classification aims to categorize objects without being constrained by predefined categories or labels. The development of CLIP [1] has made this task achievable by leveraging its

informative feature spaces. CLIP demonstrates the ability to output similar image embeddings for images belonging to the same category. Its effectiveness on various applications is vastly verified [10–13]. We utilize CLIP as our zero-shot model, complementing information lost by the memory model and maintaining open-vocabulary classification performance.

2.3 Continual learning

Continual learning strives to enable models to acquire new knowledge over time while preserving previously learned knowledge [14]. Approaches to continual learning can be broadly categorized into regularization [15–17], parameter isolation [18–22], and rehearsal methods [23–26]. Regularization techniques generally impose constraints on the learning process to alleviate forgetting. Parameter isolation methods maintain learning stability by fixing subsets of parameters [20, 21] or extending model through adding new parameters [19, 22, 27]. Rehearsal methods involve storing and replaying past data samples during training [26, 28, 29]. Our method can be considered a variant of rehearsal methods; however, instead of storing the actual images, we store image embeddings to represent past data, which helps save storage space while retaining essential information.

While prior works explore how to adapt to increasing numbers of examples, classes, or tasks, or to domain shifts, ours is the first to our knowledge to address continual learning in the context of open-vocabulary image classification, extending the capabilities of a model capable of zero-shot prediction.

3 Method

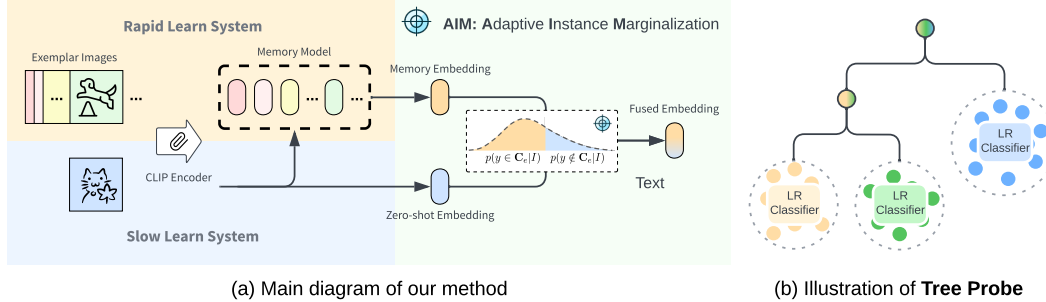


Figure 1: Illustration of our approach. (a) Our model integrates rapid and slow-learning systems. The “slow” system uses the CLIP encoder to create general embeddings from images, forming the retrieval context. The “rapid” system stores exemplars in memory, generating contextual embeddings. These two embeddings are fused by AIM via zero-shot estimation. (b) For efficiency, we propose TreeProbe as an alternative for vanilla linear probe, in which we first cluster samples through tree search and perform per-cluster linear probe.

Our approach is inspired from complimentary learning systems [2]. CLS suggests that the human brain comprises two complementary subsystems: a rapid learning system and a slow learning system, which together facilitate efficient memory storage, retrieval, and generalization. The rapid learning system forms new memories and associations quickly, allowing for the storage of unique and episodic information. The slow learning system is responsible for the gradual extraction of general knowledge and regularities across experiences. The interplay between these two complementary systems enables the brain to achieve a balance between rapid encoding of novel information and the gradual generalization of knowledge.

Analogous to CLS, our model comprises two modules: a CLIP-based base image encoder as the slow learning system, and a memory model storing extractions of images and annotations for rapid learning. We expect both modules to generate individual predictions and then fuse the outputs. In the following, we detail these modules and their fusion operations, aimed at enhancing performance for learned classes while maintaining zero-shot classification performance.

3.1 Open-vocabulary image classification

Image classification tasks in machine learning can be broadly bifurcated into **closed-set** and **open-vocabulary** scenarios. In closed-set classification, the model is trained on a finite set of known classes,

and the goal is to classify new instances into one of these predefined categories. This paradigm, however, is incapable of recognizing or accommodating classes outside of the original training set. On the other hand, open-vocabulary classification allows for a more dynamic setting in which the set of classes can be defined at inference time. This flexibility introduces new challenges but enables the same model to more easily extend or blend its learned concepts and categories. Open-vocabulary classification is typically enabled by learning a mapping from a text label to a classification vector, e.g. using a language model as in CLIP [1].

At inference time, both closed-set and open-vocabulary classification involve choosing the most probable class y_i from a candidate class set Y given an input image I . We can postulate a function f that maps I to an embedding vector e_I , represented as $e_I = f(I)$. Additionally, a per-class weight vector w_i is required to map e_I to a corresponding class logit l_i via an inner product, resulting in $l_i = w_i \cdot e_I$. These weight vectors can either be learned or contextually provided. A softmax function is subsequently used to convert logits into probabilities: $p(y = y_i | I) = \frac{\exp(l_i)}{\sum_{j=1}^n \exp(l_j)}$, $i = 1, \dots, n$ where n is the number of classes. The model finally yields the label \hat{y} with the highest probability: $\hat{y} = \arg \max_i p(y = y_i | I)$.

3.2 Slow learning system: zero-shot model

Artificial neural networks, as exemplified by foundational models such as CLIP [1], epitomize slow learning systems. Such networks learn iteratively, adjusting weights over multiple training epochs, aggregating over training data and developing increasingly abstract representations with increasing network depth. Our approach leverages the CLIP image encoder as a slow learning mechanism due to its training on a massive image-text dataset and its ability for open-vocabulary classification by comparing image encodings to text encodings. We maintain fixed CLIP encoders throughout our project, since fine-tuning degrades the model’s breadth of applicability.

Let denote the image encoder as f_{img} and the text encoder as f_{txt} . Upon receiving an input image I and a collection of textual labels $T = t_1, t_2, \dots, t_n$, the CLIP model maps I and T to their respective image and text embeddings, e_I and e_{t_i} , represented as $e_I = f_{\text{img}}(I)$, $e_{t_i} = f_{\text{txt}}(t_i)$.

Here, e_{t_i} serves a role analogous to the weight vector w_i from the previously defined classification model. The model computes logits for each class as cosine similarity between the image and text label, weighted by temperature τ (=100 in CLIP): $s(e_I, e_{t_i}) = \tau \cdot \frac{e_I \cdot e_{t_i}}{\|e_I\| \|e_{t_i}\|}$, $i = 1, \dots, n$. Thus, cosine similarity substitutes for the inner product operation prevalent in closed-set models, and the model applies a softmax function to transform logits into probabilities and selects label \hat{y} with highest probability, as in Sec 3.1.

3.3 Rapid learning system: exemplar-based memory model

For the rapid learning system, given one or more exemplars (image-label pairs), our goal is to maximize classification performance with minimal training and acceptable inference time. We consider two approaches: instance-based and model-based prediction. Instance-based prediction leverages the exemplar set directly by retrieving and comparing samples. Model-based prediction seeks to capture the underlying structure of the data through a parameterized model.

Our memory module M stores encoded image embeddings along with their text labels T . Each entry in the memory can be denoted by $M_j = \{e_{I_j}, t_j\}$ where j represents the entry index, e_{I_j} represents the image embedding of I_j , and t_j is the corresponding label.

KNN: Given e_I , the KNN memory module finds its most similar k entries in the memory through cosine similarities between e_I and all e_{I_j} in the memory. Let $\mathcal{N}_k(e_I)$ be the set of indices of the k highest cosine similarity scores to e_I . KNN classification for e_I can be performed by majority voting (MV-KNN) from the values: $\hat{y} = \arg \max_y \sum_{j \in \mathcal{N}_k(e_I)} \mathbb{1}(t_j = y)$. Here, $\mathbb{1}(\cdot)$ is an indicator function. The probability of e_I being label y_i is $p_e(y = y_i | e_I) = \frac{\sum_{j \in \mathcal{N}_k(e_I)} \mathbb{1}(t_j = y_i)}{k}$, and the label with maximum probability \hat{y} is predicted.

An alternative prediction approach is to produce a *memory* embedding, denoted as \mathbf{v}_{mem} . For the retrieved instances, we encode the text labels into text embeddings using the CLIP text encoder. We could average the retrieved text embeddings (AVG-KNN): $\mathbf{v}_{\text{mem}} = \frac{1}{k} \sum_{j \in \mathcal{N}_k(e_I)} f_{\text{txt}}(t_j)$. Related to

attention in transformers, we could also use a weighted average based on similarity (WAVG-KNN):

$$\mathbf{v}_{\text{mem}} = \sum_{j \in \mathcal{N}_k(e_I)} \beta_j \cdot f_{\text{txt}}(t_j), \text{ where } \beta_j = \frac{\exp(s(e_I, e_{I,j}))}{\sum_{j' \in \mathcal{N}_k(e_I)} \exp(s(e_I, e_{I,j'}))}.$$

KNN takes virtually no time to train ($\mathcal{O}(1)$), and reasonably fast retrieval is possible with optimized libraries and parallel computing. However, accuracy tends to be lower than model-based methods.

Linear probe: Model prediction offers an alternative approach, learning a fixed set of parameters that generalize patterns and learn the underlying structure of the data to maximize classification performance. Whenever new exemplars are added, the linear probe (LinProbe) method is to extract image embeddings and train linear classifiers on all accumulated exemplars. This relates to GDumb [30], a simple experience replay method that retrains models from scratch each time new data is received, but, to enable rapid learning, we do not retrain or fine-tune the encoder. As in CLIP [31], we use the `LogisticRegression` class from the `sklearn` library as the linear classifier.

The output probability can be written as: $p_e(y = y_i | e_I; \theta) = \frac{\exp(\theta_{y_i}^T e_I)}{\sum_{y_j \in \mathcal{C}} \exp(\theta_{y_j}^T e_I)}$, where θ_{y_i} represents the learned model parameters for label y_i . The memory embedding is the text embedding of the label \hat{y} giving the maximum probability: $\mathbf{v}_{\text{mem}} = f_{\text{txt}}(t_{\hat{y}})$.

Compared to KNN, the LinProbe model is much slower to train, $\mathcal{O}(n)$ for n training samples assuming a constant number of epochs, which may be prohibitive when the model needs to be updated quickly based on few examples. However, inference is faster than KNN, and classification accuracy tends to be higher.

Tree probe: In a continual learning setting, we would ideally have fast training time of KNN with the relatively good accuracy of LinProbe. Dusting off the older literature, we take inspiration from the instance-based and lazy learning [4], particularly locally linear models [9, 32]. These methods classify a test sample by finding its k -nearest neighbors and applying a linear classifier trained on the neighbors. This achieves $\mathcal{O}(1)$ training time but may be impractical for inference, since a new classifier may need to be trained for each test sample.

Instead, we propose an approximation, building a clustering tree from the training data and training a linear classifier in each leaf node. Starting from a root node, we search for the nearest leaf node for a new data point and insert it if the node has not reached the predefined capacity ψ ($=10000$ in our experiments). If a leaf node reaches capacity, it splits into two child nodes and becomes a non-leaf node. The attached data points are distributed to their children using KMeans clustering with two clusters. In experiments, when receiving new data, samples are added into the cluster tree one by one. Only classifiers in affected leaf node(s) need to be retrained. When fixing the number of linear model training epochs and KMeans iterations, the complexity to incorporate a new exemplar in training is $\mathcal{O}(\log n + \psi)$; the training time stays limited even when the total number of exemplars is very large.

The simplest inference method would be to assign a test sample to a leaf node in the cluster tree and classify it within the corresponding linear model, but this may lead to non-smooth predictions for samples near the cluster boundaries. In our experiments, we use an ensemble of the classifiers from leaf nodes corresponding to the k nearest neighbors for prediction. Experimentally, we find this gives a modest boost to performance with a slight increase in inference time. For each classifier c , $\theta_{y_i}^c$ represents the learned parameters for class y_i from the corresponding class set \mathcal{C}_c . The output probability is calculated by averaging the output probabilities of each classifier in $\mathcal{C}_k(e_I)$.

The memory embedding can be computed as the text embedding of the most likely label or the average text embedding for the most likely label of each classifier in the retrieval set, but we obtain the best performance using a similarity-weighted average: $\mathbf{v}_{\text{mem}} = \sum_{c \in \mathcal{C}_k(e_I)} \beta_c \cdot f_{\text{txt}}(\arg \max_{y_i \in \mathcal{C}_c} p(y = y_i | e_I; c))$, where $\beta_c = \frac{\exp(s(e_I, e_{I,c}))}{\sum_{c' \in \mathcal{C}_k(e_I)} \exp(s(e_I, e_{I,c'}))}$.

This method, denoted TreeProbe, achieves similar accuracy to LinProbe in our continual learning experiments, but with much faster training time.

3.4 Fusing predictions of the two models

We want to integrate predictions from the CLIP model and the exemplar-based memory model to retain both good open-vocabulary classification performance and high accuracy on exemplar classes. This can be tricky, especially when a subset of classes in the task are covered by the exemplar classes.

One way is to obtain an output embedding vector \mathbf{v}_{out} by averaging the zero-shot embedding e_I and memory embedding \mathbf{v}_{mem} :

$$\mathbf{v}_{\text{out}} = \alpha \mathbf{v}_{\text{mem}} + (1 - \alpha) e_I. \quad (1)$$

Then we follow the open-vocabulary classification pipeline introduced in Sec. 3.1 to obtain the final label. In design, $\alpha = 0.5$ is natural since it reflects equal confidences on zero-shot prediction and memory prediction. This simple fuse operation is called average vector (Avg-Emb).

From the probabilistic perspective, given the target class set \mathbf{C}_t , alternatively we can average probabilities from p_e and p_z . Similarly, the final probability is:

$$p(y = y_i|I) = \alpha p_e(y = y_i|I) + (1 - \alpha) p_z(y = y_i|I). \quad (2)$$

Here α is also 0.5 and we term the fuse operation Avg-Prob.

The Avg-Emb and Avg-Prob approaches presume equivalent influence of the exemplar and zero-shot models for all samples. This presumption does not hold when a test sample’s label falls within the exemplar’s domain, where the exemplar model is typically more accurate, or outside of this domain, where the zero-shot model tends to outperform.

Addressing this issue, we devise an adaptive weighting mechanism, named **Adaptive Instance Marginalization (AIM)**, that estimates the likelihood of a test sample’s label being in the exemplar set and balances the predictions from both models accordingly. The target label set is divided into exemplar $y \in \mathbf{C}_e$ and non-exemplar $y \notin \mathbf{C}_e$ subsets. The likelihoods $p(y \in \mathbf{C}_e|I)$ and $p(y \notin \mathbf{C}_e|I)$ are obtained by summing the probabilities over these subsets, with the zero-shot prediction providing a confidence metric for label set classification. Namely, $p(y \in \mathbf{C}_e|I) \propto \sum_{i \in \mathbf{C}_e} p_z(y = y_i|x)$ and $p(y \notin \mathbf{C}_e|I) \propto \sum_{i \notin \mathbf{C}_e} p_z(y = y_i|x) = 1 - p(y \in \mathbf{C}_e|I)$.

To incorporate this, we revise Eq. 1 and Eq. 2, replacing α with $p(y \in \mathbf{C}_e|I)$, resulting in two variants of fuse operations, namely AIM-Emb and AIM-Prob. This adaptive mechanism effectively capitalizes on the strengths of both prediction approaches, improving overall performance.

Since zero-shot predictions also have reasonable accuracies over exemplar classes, we also incorporate them with memory predictions for AIM-Prob:

$$p(y = y_i|I) = p(y \in \mathbf{C}_e|I) \frac{p_z(y = y_i|I) p_e(y = y_i|I)}{\sum_{j \in \mathbf{C}_e} p_z(y = y_j|I) p_e(y = y_j|I)} + p(y \notin \mathbf{C}_e|I) p_z(y = y_i|I). \quad (3)$$

This induces a slight performance improvement.

4 Experimental Setup

4.1 Tasks

In this paper, we evaluate our system through classification tasks, divided into target and zero-shot tasks based on their exposure to the memory model. We utilize **general tasks** such as ImageNet [33], SUN397 [34], CIFAR100/10 [35], Caltech101 [36], and **fine-grained tasks** like EuroSAT [37], OxfordIIITPets [38], SVHN [39], DTD [40], Flower102 [41], FGVCAircraft [42], StanfordCars [43], Food101 [44], Resisc45 [45], UCF101 [46].

Hyper-parameter searches are conducted on target tasks CIFAR10, SVHN, and Resisc45, and a zero-shot task Caltech101. For main results, to mitigate hyperparameter selection bias, we adopt different tasks: CIFAR100, SUN397, FGVCAircraft, EuroSAT, OxfordIIITPets, StanfordCars, Food101 and Flowers102 as target tasks; and ImageNet, UCF101, and DTD as zero-shot tasks. This selection, comprising both general and fine-grained tasks, more thoroughly evaluates our model’s zero-shot performance. More details including prompt templates and zero-shot performances on all tasks are provided in the supplementary materials.

4.2 Evaluation scenarios

We consider several continual learning scenarios for receiving data: 1) **Data incremental**: A fraction of the training data, randomly sampled without enforcing class balance, is added in each stage; 2) **Class incremental**: All training data for a randomly sampled subset of classes are added in each stage; 3) **Task incremental**: All data for a single task, i.e. a dataset of examples assigned to a

set of target labels, are added in each stage. Data incremental learning includes seven stages, each comprising 2%, 4%, 8%, 16%, 32%, 64%, and 100% of task data respectively. Class incremental learning divides a task into five stages, each containing 20% of classes. In task incremental learning, each task is considered a stage.

In data and class incremental experiments, models are built separately for each target task. A target task is fully evaluated if there is at least one training sample for that task, even if there are no training samples for some classes. In task incremental, one model is built spanning all of the accumulated labels in each stage. In all cases, results are reported as the average accuracy of target tasks and of a held-out zero-shot task at each stage, all normalized by baseline zero-shot accuracy.

In the task incremental setting, after all training data for target tasks is received, we also evaluate each method’s performance in several inference scenarios: **T** Target task; **Z** Zero-shot task; **U** Union of target task labels: in each task, the union of all labels is considered as valid predictions; **U-Z** Same as above, but a random sample of 100 labels from the zero-shot task are also added, and the average of target and zero-shot task performances are reported; **M** Mix of target task labels: five random splits of union of target labels are created, and average performance across splits is reported with 100 test samples per class; **M-Z** Same as above, but adding a random sample of 100 labels from the zero-shot task in each split.

4.3 Implementation details

We conduct our experiments on a setup featuring an RTX 3090 GPU and an AMD Ryzen 9 5950X CPU, using PyTorch as our primary framework. We adhere to the CLIP code example, setting the sklearn LogisticRegression regularization strength to 0.316 and the maximum iteration is set to 5K. Our tree probe’s node capacity is set at 10K. For efficient and high-speed retrievals from large-scale exemplar sets, we leverage FAISS [47], specifically using the IndexFlatIP class for its precision and performance. Model performances are gauged via Top-1 accuracy, with the officially released ViT-B/32 CLIP checkpoint serving as our memory or zero-shot model. For KNN, we set $k = 12$ for MV-KNN and $k = 6$ for other variants, based on hyperparameter tuning on the validation tasks. Additional details are provided in the supplementary materials.

5 Experimental Results

In Sec. 5.1, we compare three forms of exemplar-based memory models. We then present results of ablation experiments (Sec. 5.2), evaluating the methods of nearest neighbor blending and model fusion. Next, we evaluate with larger zero-shot backbones (Sec. 5.3), and finally present results on long-tailed classification (Sec. 5.4).

5.1 Main Results

We compare performance of the three forms of exemplar-based memory models on target tasks, zero-shot tasks, mixes, and unions (Figs. 2). We compare using only the memory models, in which zero-shot performance suffers, and fusing the zero-shot and memory models’ predictions using the **ATM-Emb** method. We consider the zero-shot model as a baseline termed as **CLIP-ZS**. We normalize the performances of different approaches with the **CLIP-ZS** to show the influence of learning, as **CLIP-ZS** is the starting point for all approaches.

We are not aware of existing works that address continual learning in an open-vocabulary image classification setting, but **WiSE-FT** [48] can be easily modified to address this problem. Initializing from a pre-trained model (image encoder and text embeddings for linear weights), such as CLIP, **WiSE-FT** fine-tunes the image encoder and/or linear model on the target data. Then, the new weights are element-wise weighted-averaged with the original weights, with a blending parameter α ($= 0.5$ by default). This method was proposed and evaluated as a way to maintain robustness to domain shift. To extend to continual learning, when new data is received, the linear model(s) for corresponding task(s) are tuned, and we replace the text embeddings for trained classes with the average ($\alpha = 0.5$) of the original embedding and the trained weights. This is similar to our **LinProbe** method and shares the disadvantage of time complexity to incorporate new data.

From Fig. 2(a-c), **LinProbe**, **TreeProbe**, and **WiSE-FT** outperform other methods across all stages. In the early stages of data and class incremental scenarios, memory-only methods struggle due to limited data. However, with more data, these methods improve and eventually surpass **CLIP-ZS**.

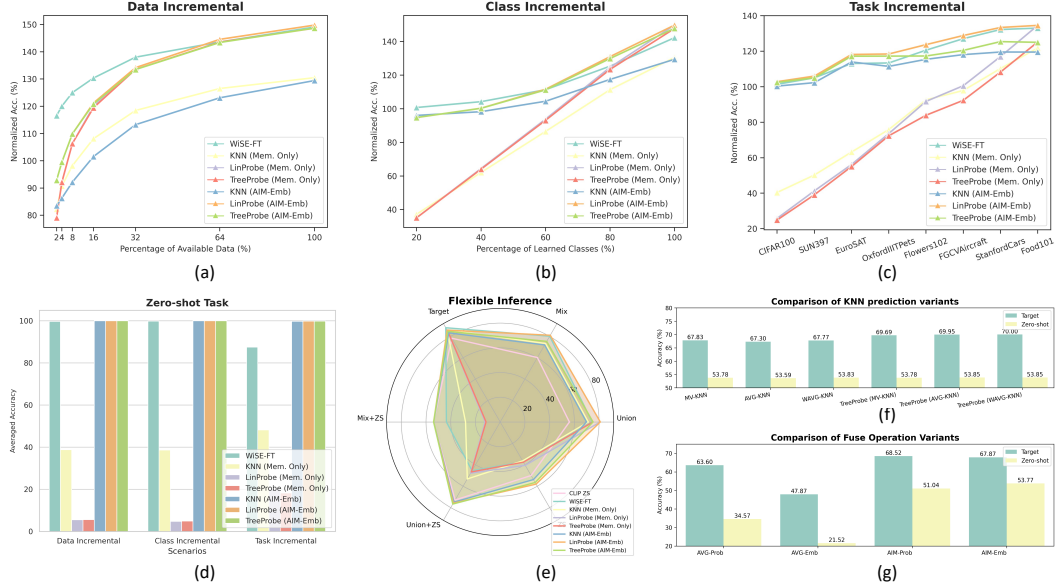


Figure 2: Results of various methods. ZS: zero-shot; FT: fine-tune; Mem. Only: only using memory model prediction without considering zero-shot model prediction. (a) Average data incremental results across eight target tasks; (b) Average class incremental results across eight target tasks; (c) Task incremental results on target tasks; (d) Average zero-shot task results across all stages on different continual learning scenarios; (e) Results of flexible inference; (f) Comparison of different KNN prediction variants in KNN and TreeProbe for target and zero-shot tasks. Performances are averaged over all stages. (g) Comparison of different fuse operations. Note: for figures (a-d), performances are normalized relative to CLIP ZS performances on both target and zero-shot tasks.

Yet, they perform subpar in zero-shot tasks, as their reliance on memory samples provides limited information for non-exemplar classes, as depicted in Fig. 2(d). With the aid of AIM, all three memory prediction methods' performance improved in zero-shot tasks, although WiSE-FT lags slightly.

The results in Fig. 2(e) show varied performance levels across tasks and models. In U, T, and M tasks, memory-only models surpass the CLIP zero-shot model, highlighting their efficacy in learned categories tasks. However, their Z task performance significantly diminishes, indicating their limitations in unseen categories. With AIM, models' Z tasks performance remarkably improves, without impacting their U, T, and M tasks performance. This underscores AIM's role in enhancing models' unseen categories handling while maintaining their learned tasks competence. WiSE-FT excels in T and M tasks but underperforms in Z and Z-involved tasks, revealing its strengths and weaknesses. LinProbe outperforms TreeProbe in U and T, with other tasks being comparable. However, TreeProbe is significantly more efficient, taking only 40 minutes to pass all stages in the task incremental setting, while LinProbe requires over 8 hours. Thus, TreeProbe when armed with AIM, provides the best balance between performance and efficiency, making it our most recommended approach.

5.2 Ablation experiments

For ablation experiments, we mainly utilize task incremental learning scenario to perform experiments as its domain shift is larger than other scenarios, being more challenging. More experiment results are in supplementary materials including selection of k .

Comparison of variants of KNN prediction In Sec. 3.3, we illustrate three variants of KNN prediction approaches, namely MV-KNN, AVG-KNN and WAVG-KNN. As TreeProbe also involves the procedure of aggregating results from the k nearest classifiers, we also experiment on the TreeProbe approach. We report averaged accuracy for both target tasks and zero-shot tasks by averaging across all stages. In Fig. 2(f), we can read that MV-KNN is the best for KNN predictions and WAVG-KNN is the best for TreeProbe prediction.

Comparison of variants of fuse operations As delineated in Sec. 3.4, we propose four fusion operations: Avg-Prob, Avg-emb, AIM-Prob, and AIM-Emb. Experimental results, averaged across stages and depicted in Fig. 2(g), validate our choice of AIM-Emb as the optimal fusion operation. This selection is based on the superior performance of AIM variants over Avg ones, particularly noticeable in both target and zero-shot tasks. Despite AIM-Emb showing marginally lower target performance compared to AIM-Prob, it confers distinct advantages in zero-shot tasks. We thus employ AIM for blending predictions from the zero-shot model and the memory model, averaging the embeddings to achieve overall enhanced performance.

5.3 Scaling to better zero-shot models

Method	ViT-B/32		ViT-L/14@336px		ViT-H/14	
	Target	Zero-shot	Target	Zero-shot	Target	Zero-shot
CLIP ZS	60.2	54.0	72.1	65.6	79.2	71.7
TreeProbe (AIM-Emb)	70.0	53.9	81.4	65.5	85.2	71.6

Table 1: Accuracies of CLIP ZS and TreeProbe on target and zero-shot tasks with pretrained image encoders of different capacities.

We default to using the CLIP ViT-B-32 model as our zero-shot model, but our approach is adaptable to any open-vocabulary foundational models. It can be effortlessly upgraded to superior models by simply swapping the zero-shot model. To demonstrate this, we experiment with the more advanced pretrained CLIP model ViT-L/14@336px, which boasts approximately 4x the capacity of ViT-B/32, and ViT-H/14², which is double the size of ViT-L/14@336px. As zero-shot performance on ImageNet improves with larger capacities, we present our findings in Tab. 1. By shifting to more advanced models, both CLIP ZS and TreeProbe have performance improvements, and TreeProbe also consistently outperforms CLIP ZS, demonstrating how our approach benefits from the enhanced capacity of zero-shot models.

5.4 Evaluation on long-tailed classification

Method	CLIP ZS	KNN	LinProbe	TreeProbe	KNN*	LinProbe*	TreeProbe*	PaCo [49]	RAC [50]
Accuracy (%)	40.0	35.5	37.0	30.5	40.4	42.7	41.3	41.2	47.2

Table 2: Comparison of long-tailed classification on Places365LT [51]. * means + AIM-Emb. Note for this experiment, we utilize CLIP ViT-L/14@336px as the backbone network.

As shown in RAC [50], their framework has superior performance on long-tailed classification, demonstrating the retrieval procedure provides benefits to tail classes. Likewise, in addition to the continual learning settings, we explore the possibilities of extending our method for long-tailed classification. Specifically, we note the zero-shot model’s proficiency in distinguishing *tail* classes, while the memory model exhibits superior accuracy for *head* classes. Following this, we categorize classes into tail (C_{tail}) and head (C_{head}) based on their sample sizes, designating the bottom two-thirds as *tail*. Then, in line with the AIM approach, we amalgamate the zero-shot (e_I) and memory (v_{mem}) embeddings, using the probability of a sample’s affiliation to either the head or tail class, to produce the output embedding: $v_{out} = p(y \in C_{head}|I)v_{mem} + p(y \in C_{tail}|I)e_I$. Here, $p(y \in C_{head}|I) \propto \sum_{i \in C_{head}} p_z(y = y_i|x)$ and $p(y \in C_{tail}|I) = 1 - p(y \in C_{head}|I)$.

Accuracy on the Places365LT dataset [51] is presented in Tab. 2. These results demonstrate that all three memory prediction approaches, when enhanced with AIM, outperform their respective versions without AIM. Compared to recent works specifically designed for long-tailed recognition, our method performs similarly to PaCo [49], while RAC achieves moderately higher accuracy.

6 Conclusion and limitations

Our work has several **limitations**. First, we do not consider memory constraints. Since each exemplar requires storing up to 4KB for the image and text encodings (using the base CLIP model without any compression or limiting precision), roughly one million exemplars can be stored per 4GB of memory. Second, we do not consider how to improve the consolidated zero-shot model using the exemplars. Finally, we do not consider structured prediction problems like semantic segmentation or visual question answering, in which the notion of exemplar may need to be redefined.

²Checkpoint from https://github.com/mlfoundations/open_clip

In this work, we present an efficient and performant “tree probe” method for open-vocabulary continual learning. We also devise a strategy to combine zero-shot and memory models, which is also shown useful for long-tailed classification. Our flexible system, thoroughly tested on challenging scenarios, readily expands capabilities while leveraging advanced zero-shot models with minimal effort. We hope this work represents a step towards flexible, efficient, and powerful strategies in open-vocabulary continual learning.

References

- [1] Alec Radford, Jong Wook Kim, Chris Hallacy, Aditya Ramesh, Gabriel Goh, Sandhini Agarwal, Girish Sastry, Amanda Askell, Pamela Mishkin, Jack Clark, et al. Learning transferable visual models from natural language supervision. In *Proc. ICML*, 2021.
- [2] Howard MD Ketz N O'Reilly RC, Bhattacharyya R. Complementary learning systems. *Cognitive Science*, 38(6):1229–1248, 2014.
- [3] Gianluca Bontempi, Mauro Birattari, and Hugues Bersini. Lazy learning for local modelling and control design. *International Journal of Control*, 72(7-8):643–658, 1999.
- [4] Charu C. Aggarwal. Instance-based learning : A survey. In *Data Classification: Algorithms and Applications*, chapter 6. CRC Press, 2014.
- [5] Gongde Guo, Hui Wang, David Bell, Yixin Bi, and Kieran Greer. Knn model-based approach in classification. In *On The Move to Meaningful Internet Systems 2003: CoopIS, DOA, and ODBASE: OTM Confederated International Conferences, CoopIS, DOA, and ODBASE 2003, Catania, Sicily, Italy, November 3-7, 2003. Proceedings*, pages 986–996. Springer, 2003.
- [6] Hao Zhang, Alexander C Berg, Michael Maire, and Jitendra Malik. Svm-knn: Discriminative nearest neighbor classification for visual category recognition. In *2006 IEEE Computer Society Conference on Computer Vision and Pattern Recognition (CVPR'06)*, volume 2, pages 2126–2136. IEEE, 2006.
- [7] Shichao Zhang, Xuelong Li, Ming Zong, Xiaofeng Zhu, and Debo Cheng. Learning k for knn classification. *ACM Transactions on Intelligent Systems and Technology (TIST)*, 8(3):1–19, 2017.
- [8] Yunsheng Song, Jiye Liang, Jing Lu, and Xingwang Zhao. An efficient instance selection algorithm for k nearest neighbor regression. *Neurocomputing*, 251:26–34, 2017.
- [9] Christopher G. Atkeson, Andrew W. Moore, and Stefan Schaal. Locally weighted learning. *Artificial Intelligence Review*, 11:11–73, 1997.
- [10] Mitchell Wortsman, Gabriel Ilharco, Jong Wook Kim, Mike Li, Simon Kornblith, Rebecca Roelofs, Raphael Gontijo Lopes, Hannaneh Hajishirzi, Ali Farhadi, Hongseok Namkoong, et al. Robust fine-tuning of zero-shot models. In *Proceedings of the IEEE/CVF Conference on Computer Vision and Pattern Recognition*, pages 7959–7971, 2022.
- [11] Xiuye Gu, Tsung-Yi Lin, Weicheng Kuo, and Yin Cui. Open-vocabulary object detection via vision and language knowledge distillation. *arXiv preprint arXiv:2104.13921*, 2021.
- [12] Golnaz Ghiasi, Xiuye Gu, Yin Cui, and Tsung-Yi Lin. Open-vocabulary image segmentation. *arXiv preprint arXiv:2112.12143*, 2021.
- [13] Ziyi Lin, Shijie Geng, Renrui Zhang, Peng Gao, Gerard de Melo, Xiaogang Wang, Jifeng Dai, Yu Qiao, and Hongsheng Li. Frozen clip models are efficient video learners. In *Computer Vision–ECCV 2022: 17th European Conference, Tel Aviv, Israel, October 23–27, 2022, Proceedings, Part XXXV*, pages 388–404. Springer, 2022.
- [14] Michael McCloskey and Neal J Cohen. Catastrophic interference in connectionist networks: The sequential learning problem. In *Psychology of learning and motivation*, volume 24, pages 109–165. Elsevier, 1989.
- [15] Zhizhong Li and Derek Hoiem. Learning without forgetting. In *Proc. ECCV*, 2016.
- [16] James Kirkpatrick, Razvan Pascanu, Neil C. Rabinowitz, Joel Veness, Guillaume Desjardins, Andrei A. Rusu, Kieran Milan, John Quan, Tiago Ramalho, Agnieszka Grabska-Barwinska, Demis Hassabis, Claudia Clopath, Dharshan Kumaran, and Raia Hadsell. Overcoming catastrophic forgetting in neural networks. *CoRR*, abs/1612.00796, 2016.
- [17] Friedemann Zenke, Ben Poole, and Surya Ganguli. Continual learning through synaptic intelligence. pages 3987–3995, 2017.

[18] Rahaf Aljundi, Punarjay Chakravarty, and Tinne Tuytelaars. Expert gate: Lifelong learning with a network of experts. In *CVPR*, pages 7120–7129, 2017.

[19] Andrei A. Rusu, Neil C. Rabinowitz, Guillaume Desjardins, Hubert Soyer, James Kirkpatrick, Koray Kavukcuoglu, Razvan Pascanu, and Raia Hadsell. Progressive neural networks. *arXiv:1606.04671*, 2016.

[20] Joan Serrà, Didac Suris, Marius Miron, and Alexandros Karatzoglou. Overcoming catastrophic forgetting with hard attention to the task. pages 4555–4564, 2018.

[21] Arun Mallya and Svetlana Lazebnik. Packnet: Adding multiple tasks to a single network by iterative pruning. In *CVPR*, 2018.

[22] Jeffrey O. Zhang, Alexander Sax, Amir Zamir, Leonidas J. Guibas, and Jitendra Malik. Side-tuning: A baseline for network adaptation via additive side networks. In *ECCV*, pages 698–714, 2020.

[23] Sylvestre-Alvise Rebuffi, Alexander Kolesnikov, Georg Sperl, and Christoph H. Lampert. icarl: Incremental classifier and representation learning. In *Proc. CVPR*, 2017.

[24] Shipeng Yan, Jiangwei Xie, and Xuming He. DER: dynamically expandable representation for class incremental learning. In *Proc. CVPR*, 2021.

[25] David Lopez-Paz and Marc’Aurelio Ranzato. Gradient episodic memory for continual learning. In *Proc. NeurIPS*, 2017.

[26] Hanul Shin, Jung Kwon Lee, Jaehong Kim, and Jiwon Kim. Continual learning with deep generative replay. In *NeurIPS*, pages 2990–2999, 2017.

[27] Jaehong Yoon, Eunho Yang, Jeongtae Lee, and Sung Ju Hwang. Lifelong learning with dynamically expandable networks. *arXiv preprint arXiv:1708.01547*, 2017.

[28] Rich Caruana. Multitask learning. *Machine learning*, 28:41–75, 1997.

[29] Jihwan Bang, Heesu Kim, Youngjoon Yoo, Jung-Woo Ha, and Jonghyun Choi. Rainbow memory: Continual learning with a memory of diverse samples. In *CVPR*, pages 8218–8227, 2021.

[30] Ameya Prabhu, Philip Torr, and Puneet Dokania. Gdumb: A simple approach that questions our progress in continual learning. In *The European Conference on Computer Vision (ECCV)*, August 2020.

[31] Alec Radford, Jong Wook Kim, Chris Hallacy, Aditya Ramesh, Gabriel Goh, Sandhini Agarwal, Girish Sastry, Amanda Askell, Pamela Mishkin, Jack Clark, Gretchen Krueger, and Ilya Sutskever. Learning transferable visual models from natural language supervision. In *ICML*, 2021.

[32] C. Domeniconi and D. Gunopulos. Adaptive nearest neighbor classification using support vector machines. In *NeurIPS*, 2002.

[33] Olga Russakovsky, Jia Deng, Hao Su, Jonathan Krause, Sanjeev Satheesh, Sean Ma, Zhiheng Huang, Andrej Karpathy, Aditya Khosla, Michael S. Bernstein, Alexander C. Berg, and Li Fei-Fei. Imagenet large scale visual recognition challenge. *IJCV*, 115(3):211–252, 2015.

[34] Jianxiong Xiao, James Hays, Krista A Ehinger, Aude Oliva, and Antonio Torralba. Sun database: Large-scale scene recognition from abbey to zoo. In *Proc. CVPR*, 2010.

[35] Alex Krizhevsky, Geoffrey Hinton, et al. Learning multiple layers of features from tiny images. 2009.

[36] Fei-Fei Li, Marco Andreetto, Marc’Aurelio Ranzato, and Pietro Perona. Caltech 101, 2022.

[37] Patrick Helber, Benjamin Bischke, Andreas Dengel, and Damian Borth. Eurosat: A novel dataset and deep learning benchmark for land use and land cover classification. *IEEE Journal of Selected Topics in Applied Earth Observations and Remote Sensing*, 2019.

[38] Omkar M. Parkhi, Andrea Vedaldi, Andrew Zisserman, and C. V. Jawahar. Cats and dogs. In *Proc. CVPR*, 2012.

[39] Yuval Netzer, Tao Wang, Adam Coates, Alessandro Bissacco, Bo Wu, and Andrew Y Ng. Reading digits in natural images with unsupervised feature learning. 2011.

[40] M. Cimpoi, S. Maji, I. Kokkinos, S. Mohamed, , and A. Vedaldi. Describing textures in the wild. In *Proc. CVPR*, 2014.

- [41] Maria-Elena Nilsback and Andrew Zisserman. Automated flower classification over a large number of classes. In *2008 Sixth Indian Conference on Computer Vision, Graphics & Image Processing*, 2008.
- [42] Subhransu Maji, Esa Rahtu, Juho Kannala, Matthew Blaschko, and Andrea Vedaldi. Fine-grained visual classification of aircraft. *arXiv preprint arXiv:1306.5151*, 2013.
- [43] Jonathan Krause, Michael Stark, Jia Deng, and Li Fei-Fei. 3d object representations for fine-grained categorization. In *4th International IEEE Workshop on 3D Representation and Recognition (3dRR-13)*, 2013.
- [44] Lukas Bossard, Matthieu Guillaumin, and Luc Van Gool. Food-101 – mining discriminative components with random forests. In *European Conference on Computer Vision*, 2014.
- [45] Gong Cheng, Junwei Han, and Xiaoqiang Lu. Remote sensing image scene classification: Benchmark and state of the art. *Proceedings of the IEEE*, (10), 2017.
- [46] Khurram Soomro, Amir Roshan Zamir, and Mubarak Shah. UCF101: A dataset of 101 human actions classes from videos in the wild. *CoRR*, abs/1212.0402, 2012.
- [47] Jeff Johnson, Matthijs Douze, and Hervé Jégou. Billion-scale similarity search with GPUs. *IEEE Transactions on Big Data*, 2019.
- [48] Mitchell Wortsman, Gabriel Ilharco, Jong Wook Kim, Mike Li, Simon Kornblith, Rebecca Roelofs, Raphael Gontijo Lopes, Hannaneh Hajishirzi, Ali Farhadi, Hongseok Namkoong, and Ludwig Schmidt. Robust fine-tuning of zero-shot models. In *CVPR*, pages 7949–7961, 2022.
- [49] Jiequan Cui, Zhisheng Zhong, Shu Liu, Bei Yu, and Jiaya Jia. Parametric contrastive learning. In *ICCV*, pages 695–704, 2021.
- [50] Alexander Long, Wei Yin, Thalaiyasingam Ajanthan, Vu Nguyen, Pulak Purkait, Ravi Garg, Alan Blair, Chunhua Shen, and Anton van den Hengel. Retrieval augmented classification for long-tail visual recognition. In *Proc. CVPR*, 2022.
- [51] Ziwei Liu, Zhongqi Miao, Xiaohang Zhan, Jiayun Wang, Boqing Gong, and Stella X. Yu. Large-scale long-tailed recognition in an open world. In *CVPR*, pages 2537–2546, 2019.
- [52] Ameya Prabhu, Hasan Abed Al Kader Hammoud, Puneet K. Dokania, Philip H. S. Torr, Ser-Nam Lim, Bernard Ghanem, and Adel Bibi. Computationally budgeted continual learning: What does matter? *CoRR*, abs/2303.11165, 2023.
- [53] Bolei Zhou, Àgata Lapedriza, Aditya Khosla, Aude Oliva, and Antonio Torralba. Places: A 10 million image database for scene recognition. *IEEE TPAMI*, 40(6):1452–1464, 2018.

A Supplementary materials

A.1 Algorithmic descriptions of TreeProbe

Algorithm 1: Training Procedure of TreeProbe

Input: Training set X , Tree T , Leaf capacity ψ
Output: Trained classifiers in each leaf node of T

```

foreach  $x_i \in X$  do
     $l = \text{NEARESTLEAF}(x_i, T)$ 
    if  $\text{CAPACITY}(l) < \psi$  then
         $l = \text{INSERTDATA}(x_i, l)$ 
         $\text{TRAINCLASSIFIER}(l)$ 
    end
    else
         $\text{SPLITNODE}(l, x_i)$ 
         $l = \text{NEARESTLEAF}(x_i, T)$ 
         $l = \text{INSERTDATA}(x_i, l)$ 
         $\text{TRAINCLASSIFIER}(l)$ 
    end
end

```

Algorithm 2: Inference Procedure of TreeProbe

Input: Test sample x_j , Tree T , Number of nearest nodes k
Output: Memory embedding \mathbf{v}_{mem} for x_j

```

 $\mathcal{L} = \text{FINDNEARESTNODES}(x_j, T, k)$ 
foreach  $l \in \mathcal{L}$  do
     $\text{CLASSIFY}(x_j, l)$ 
end
 $\mathbf{v}_{\text{mem}} = \text{COMPUTEMBEDDING}(x_j, \mathcal{L})$ 

```

In Algorithm 1 and Algorithm 2, we utilize algorithmic language to elucidate the training and inference processes of TreeProbe, enhancing its comprehensibility. Definitions of the involved functions are provided below:

- **NEARESTLEAF**(x_i, T): Returns the nearest leaf node to the data point x_i in tree T .
- **CAPACITY**(l): Returns the current number of data points in leaf node l .
- **INSERTDATA**(x_i, l): Inserts data point x_i into leaf node l and returns the updated node.
- **SPLITNODE**(l, x_i): Splits leaf node l into two child nodes when it reaches capacity, distributes data points using KMeans clustering, and adds new data point x_i to the appropriate child node.
- **TRAINCLASSIFIER**(l): Trains a linear classifier on the data points in leaf node l .
- **FINDNEARESTNODES**(x_j, T, k): Finds the k leaf nodes in tree T nearest to the test sample x_j .
- **CLASSIFY**(x_j, l): Classifies test sample x_j using the linear classifier in leaf node l , returning the output probabilities for each class.
- **COMPUTEMBEDDING**(x_j, \mathcal{L}): Computes the memory embedding for test sample x_j by applying a similarity-weighted average of the text embeddings of the most likely class labels from the classifiers in the set of nodes \mathcal{L} .

Note that we re-purpose several denotations from the main paper in Algorithm 1 and Algorithm 2 for better clarity.

A.2 Additional implementation details

More main comparison details When evaluating different methods in data and class incremental learning scenarios, we ensure fairness by randomly selecting an identical portion of data/class for all methods, achieved by setting the same seed. The performance of each stage is averaged across all target tasks. In task-incremental learning, each stage is embodied by a distinct task, with the assumption that training data accumulates across all stages in all scenarios, similar to [52]. This assumption is based on the fact that real-world applications are often more limited by computational and time budgets than by storage. Furthermore, we enhance storage efficiency by saving samples as

condensed feature vectors, a significant improvement over some earlier works. The results for KNN (Mem. Only) in Fig. 2 in the main paper are referred to as MAVG-KNN.

More scaling zero-shot model details For experiments in Sec. 5.3, we follow ablation experiments to utilize task incremental learning setting to test the average target and zero-shot accuracies of different backbones across all stages.

More flexible inference details

- **T** performance averages results over all target tasks, considering only task-specific labels as potential outputs.
- **Z** is evaluated similarly to **T** but operated on zero-shot tasks.
- For **U**, an union of all target tasks is created for evaluation, with classification options consisting of all task labels combined.
- **U-Z** averages the performance over **U** and **Z**, with classification options including a union of all task labels and 100 zero-shot labels.
- **M** evaluates performance over 5 splits of the union task and reports the average score.
- Similar to **U-Z**, **M-Z** adds 100 random zero-shot task labels to each split, expanding classification options to include each split’s union and an additional 100 zero-shot labels.

A.3 Intuitive demonstration of evaluation scenarios

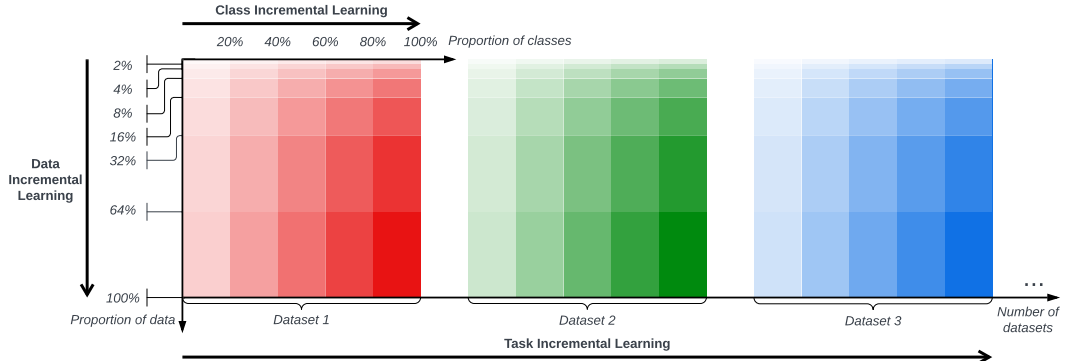


Figure 3: Illustration of continual learning scenarios. Data incremental learning includes seven stages, each comprising 2%, 4%, 8%, 16%, 32%, 64%, and 100% of task data respectively. Class incremental learning divides a task into five stages, each containing 20% of classes. In task incremental learning, each task is considered a stage. For data and class incremental scenarios, we run experiments under each target task and average the performances of each stage across different tasks. For task incremental scenario, however, we run through all tasks and treat each task as an individual task.

A.4 Descriptions of tasks

We perform experiments on a variety of commonly-used visual datasets to demonstrate the generalization capabilities of our method. These datasets encompass a broad range of image categories and application scenarios, including both fine-grained and generalized datasets. We present a brief introduction to all used tasks in this paper in the following.

A.4.1 General tasks

ImageNet ImageNet [33] contains 1,281,167 training images, 50,000 validation images and 100,000 test images. The categories represent a wide variety of objects, animals, scenes, and even abstract concepts. This dataset has served as a fundamental dataset to evaluate performances of classification models, or as a pretraining dataset.

CIFAR100 The CIFAR100 dataset [35] consists of object images and is a subset of the 80 million tiny images dataset. It contains 60,000 32×32 color images from 100 object categories, with 600 images per category. The dataset has 100 fine-grained classes, grouped into 20 coarse-grained classes.

CIFAR10 The CIFAR10 dataset [35] is a subset of the 80 million tiny images dataset, just like CIFAR100. However, it is significantly smaller, containing 60,000 32×32 color images from 10 distinct categories, with 6,000 images per category. The categories include objects such as cars, birds, cats, and trucks. The dataset has a balanced distribution of images across categories and is frequently used as a benchmark in machine learning research for image classification tasks.

Caltech101 The Caltech101 dataset [36] is a widely used benchmark for object recognition. It features images of objects from 101 categories, ranging from 40 to 800 images per category. Caltech-101 is a more general dataset compared to FGVCAircraft, StanfordCars, and Flowers102.

SUN397 The SUN397 dataset [34] consists of scene images, containing 108,754 images across 397 scene categories, with each category having between 100 and 500 images. This dataset is commonly used for scene understanding tasks.

A.4.2 Fine-grained tasks

FGVCAircraft The FGVCAircraft dataset [42] serves as a benchmark for fine-grained visual categorization of aircraft. It contains 10,200 images from 102 distinct categories. Each category includes approximately 100 images, annotated with the aircraft model, variant, and manufacturer.

DTD The Describable Textures Dataset (DTD) [40] consists of 5,640 images across 47 texture categories, with each category featuring 120 real-world texture images such as fabrics, rocks, and surfaces. The dataset poses a challenge for texture classification due to subtle differences between textures within the same category and large variations in texture appearance caused by scale, orientation, and lighting.

StanfordCars The StanfordCars dataset [43] is a benchmark dataset containing 16,185 images from 196 different car classes, divided into a 50-50 training and testing split. The classes correspond to specific car makes, models, and years, such as the 2012 Tesla Model S or 2012 BMW M3 coupe.

Flowers102 The 102 Category Flower Dataset [41] is a compilation of flower images. It includes 8,189 images across 102 flower categories, with each category containing between 40 and 258 images. The dataset's images vary in size and aspect ratio, captured using different cameras, lighting conditions, and backgrounds.

OxfordIIITPets The OxfordIIITPets dataset [38] is a collection of pet images, featuring 7,349 images from 37 different cat and dog breeds. Each breed has between 100 and 200 images. The dataset is challenging because the appearance of the same breed can vary significantly, and different breeds may have similar-looking features.

SVHN The Street View House Numbers (SVHN) [39] dataset is a collection of house number images. It includes 732,000 images of house numbers in various settings, such as street views, storefronts, and building facades. The dataset is frequently used for digit recognition tasks.

EuroSAT The EuroSAT dataset [37] is a remote sensing image dataset comprising Sentinel-2 satellite data. It contains 27,000 images that cover 13 spectral bands and consist of 10 different land use and land cover categories, including forests, urban areas, and water bodies. This dataset is commonly employed for remote sensing and land cover classification tasks.

Resisc45 The Remote Sensing Image Scene Classification (Resisc45) dataset [45] is a comprehensive dataset for remote sensing image scene classification. It comprises 31,500 images, with 700 images from 45 different scene categories. The categories encompass a broad range of natural and man-made scenes such as airports, beaches, forests, and residential areas. The images are collected from Google Earth and are in RGB format with a size of 256×256 pixels. This dataset poses a challenge due to large within-class variations and between-class similarities.

UCF101 The UCF101 dataset [46] is a commonly used benchmark for action recognition. It consists of 13,320 videos from 101 action categories, with each category containing at least 100 videos. The actions include a wide range of human activities such as basketball shooting, horse riding, and juggling. The dataset is unique in its focus on complex, naturalistic action sequences, with videos varying in length from a few seconds to a minute.

A.4.3 Long-tailed task

Places365LT Places365LT [51] a synthetic long-tail derivative of Places2 dataset [53]. The image resolution is 256×256 . It contains 365 scene classes with at least 5 samples each. The classes are not uniformly distributed, forming a long-tailed distribution. It contains some label noises, making classification even harder on this dataset.

A.5 Prompt templates for tasks

Task(s)	Prompt template
ImageNet [33], CIFAR10/100 [35], Caltech101 [36], SUN397 [34]	“a photo of a {label}.”
FGVCAircraft [42]	“a photo of a {label}, a type of aircraft.”
DTD [40]	“a photo of a {label} texture.”
StanfordCars [43]	“a photo of a {label}, a type of car.”
Flowers102 [41]	“a photo of a {label}, a type of flower.”
OxfordIIITPets [38]	“a photo of a {label}, a type of pet.”
SVHN [39]	“a photo of the number: “{label}”.”
EuroSAT [37]	“a centered satellite photo of {label}.”
Resisc45 [45]	“satellite photo of {label}.”
UCF101 [38]	“a video of a person doing {label}.”
Places365LT [51]	“a photo of the {label}, a type of place.”

Table 3: Prompts of tasks

CLIP [1] suggests utilizing a sentence template (e.g., “A photo of a {label}.”), as input to the text decoder instead of a plain text label, due to its training data being primarily full sentences describing images. Consistent with the focus of this paper, we employ simple prompt template for each task. Most of these templates are based on CLIP’s recommendations³ and are summarized in Tab. 3.

A.6 Zero-shot performances on different tasks

Task	Zero-shot Acc (%)	Official ZS Acc (%)
ImageNet [33]	59.7	63.2
CIFAR100 [35]	62.3	65.1
CIFAR10 [35]	88.3	91.3
Caltech101 [36]	83.6	87.9
SUN397 [34]	59.2	63.2
FGVCAircraft [42]	18.1	21.2
DTD [40]	42.0	44.5
StanfordCars [43]	58.6	59.4
Flowers102 [41]	67.9	66.7
OxfordIIITPets [38]	87.5	87.0
SVHN [39]	31.6	/
EuroSAT [37]	45.4	49.4
Resisc45 [45]	54.7	60.3
UCF101 [38]	60.1	64.5
Places365LT [51]	40.0	/

Table 4: Zero-shot performances of CLIP ViT-B/32 pretrained model on different tasks. “ZS” is for zero-shot and “Acc” is for accuracy. Results of column “Official ZS Acc” are taken from the CLIP original paper [1]. “/” represents lack of official results.

Tab. 4 shows the zero-shot performance of our implementation in different tasks. The main difference of official zero-shot performances comes from the ensemble prompt trick as mentioned in CLIP [1].

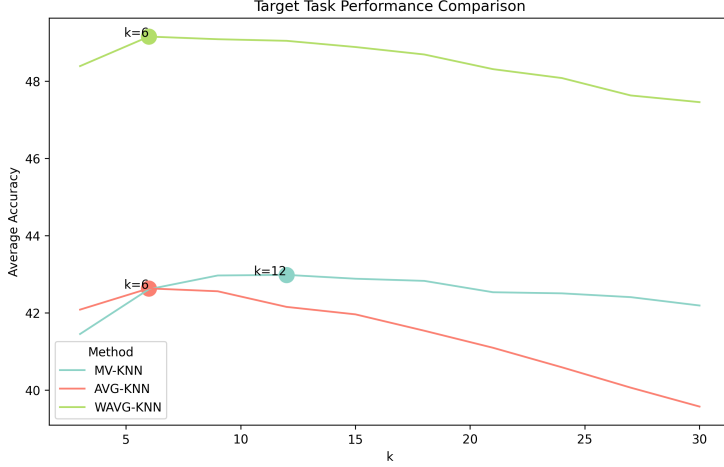


Figure 4: k selection experiments based on target performances averaged across different stages when evaluated using task incremental learning scenario. We mark the k values of the maximum accuracies of all methods.

A.7 Additional ablation experiments

k selection KNN and TreeProbe prediction approaches rely on retrieving the nearest k exemplars to make predictions, thus being influential to the performance. To select the best k , we experiment on memory-only approaches by varying k with an interval of 3. As indicated in Fig. 4, from the curve, MV-KNN achieves the best result when $k = 12$ while MAVG-KNN performs best at $k = 6$. Optimal k is found relatively larger for MV-KNN since a smaller k may filter out correct answer from the retrievals but larger k would include more mismatches from the nearest neighbors, especially when some classes are not balanced in sample number. From the plot, we can clearly read that MAVG-KNN is consistently better than AVG-KNN and MV-KNN across different k s, making it our default option when using KNN as the prediction approach for rapid learning system.

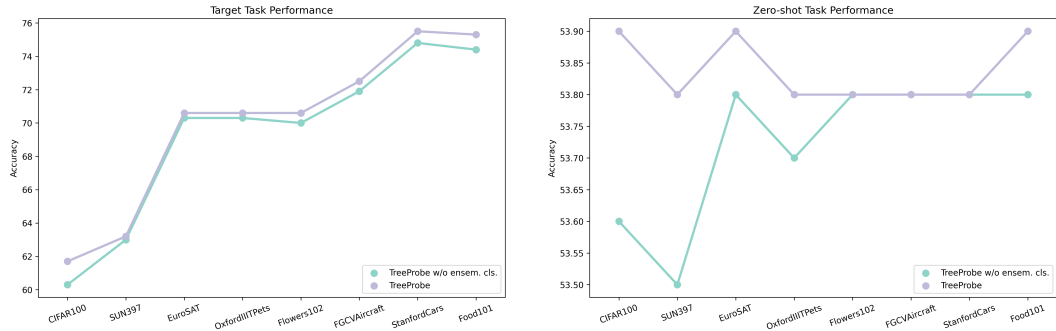


Figure 5: Target and zero-shot task performance comparison w.r.t. ensemble classifiers. “TreeProbe w/o ensem. cls.” is the version of TreeProbe by finding the cluster most similar to the input and using the corresponding classifier to predict labels.

Effect of ensemble classifiers in TreeProbe inference Referencing Sec. 3.3, we observe that ensemble predictions from multiple classifiers associated with k retrievals enhance performance. Fig. 5 presents these results under the task incremental learning setting for eight target tasks. Our final model, TreeProbe, outperforms its variant without the ensemble classification function in both target and zero-shot performance, confirming the efficacy of this technique.

³<https://github.com/openai/CLIP/blob/main/data/prompts.md>

A.8 Detailed time analysis

Tab. 5 compares the time complexity and actual times of three prediction approaches in a rapid learning system: KNN, LinProbe, and TreeProbe. The actual times are calculated in a task incremental learning scenario, with k set to 6.

KNN has a constant time complexity for both training and inference, with actual times of 9.8 and 416.1 seconds respectively. LinProbe has linear training time complexity and constant inference time complexity. The actual training time is considerably long at 30971.4 seconds (~ 8.6 hours), and the inference time is 449.1 seconds. Our most recommended algorithm, TreeProbe, has logarithmic training time complexity and linear inference time complexity related to the number of retrieved classifiers (k). In practice, it exhibits significantly shorter training time than LinProbe at 2082.0 seconds (~ 0.6 hour) while having a slight increase in inference time. The table illustrates that TreeProbe strikes a balance between accuracy and efficiency, being more accurate than KNN and more efficient than LinProbe. Note that numbers may vary depending on software and hardware situations. This number is collected from the same PC we used to run all experiments.

Methods	Train time	Inference time	Actual TT (s)	Actual IT (s)
KNN	$\mathcal{O}(1)$	$\mathcal{O}(n)$	9.8	416.1
LinProbe	$\mathcal{O}(n)$	$\mathcal{O}(1)$	30971.4	449.1
TreeProbe	$\mathcal{O}(\log n + \phi)$	$\mathcal{O}(k)$	2082.0	614.1

Table 5: Time analysis of different prediction approaches in rapid learning system, namely KNN, LinProbe, TreeProbe. Here, k represents the number of retrieved classifiers. “TT” means training time while “IT” means inference time. Actual train and inference time is calculated with task incremental learning scenario by summing up time spend on training and inference across all tasks. For TreeProbe, $k = 6$.